Network 2 (1991) 245–258. Printed in the UK

Realistic synaptic inputs for model neural networks

L F Abbott

Physics Department and Center for Complex Systems, Brandeis University, Waltham, MA 02254, USA

Received 27 March 1991

Abstract. An expression is derived relating the input current for a single neuron in a neural network to the firing rates of excitatory and inhibitory inputs synapsing on the dendritic tree of the neuron. Any dendritic geometry and any pattern of synaptic connections can be treated using the techniques presented. The input currents calculated, combined with known firing rate functions, allow the effects of synaptic conductance changes along dendritic cables to be included in a mean-field description of network behaviour. The shunting effects of inhibitory synaptic conductances provide a solution to the high firing rate problem in neutral network models

1. Introduction

Neural network models are often based on a mean-field approach [1] that uses known properties of single neurons to predict the behaviour of large neuronal populations In such models, the average firing rates of excitatory and inhibitory neurons are used to describe the activity of the population. The basic equations of mean-field theory relate these average rates to the rate of firing of a single neuron expressed as a function of its input current The equations become a closed system when the input current is expressed in turn as a function of the average firing rates for the population In a laboratory setting, the rate of single-neuron firing for various input currents can be measured by injecting current directly into the soma through a microelectrode. However, to use this firing rate in a network setting, we need to know the amount of current flowing into the soma from synaptic inputs as a function of the firing rates of presynaptic excitatory and inhibitory neurons. This information is much more difficult to obtain.

In neural network models, the input current is generally taken to be a linear function of the excitatory and inhibitory input firing rates. This approximation leaves out several essential features of real synaptic inputs and real dendritic trees. The arrival of an action potential at a presynaptic terminal results in a change in the membrane conductance on the postsynaptic side. The total synaptic conductance due to many synaptic inputs is an approximately linear function of the input firing rate, but this does not imply that injected current is linear in the firing rate. Even for quite low input firing rates, the synaptic conductance may be comparable to or even larger than the membrane conductance in the absence of synaptic inputs. When synaptic conductances make an appreciable contribution to the total membrane conductance, the dependence of somatic input current on presynaptic firing rates becomes nonlinear. The nonlinear effects of inhibition due to membrane conductance changes have been

0954-898X/91/030245+14$03.50

discussed elsewhere [2–5] but have not previously been incorporated into network models.

Currents entering through dendritic synapses must travel down dendritic cables before reaching the soma They are thus subject to losses from the longitudinal resistance of the dendritic cable and due to leakage through the dendritic membrane. Since synaptic conductances along the dendritic cable dramatically affect the amount of membrane leakage, they have an important nonlinear impact on the amount of current entering the soma. The effect depends on both the geometry of the dendritic tree and on the placement of synapses along the tree. The linear relation used in neural network models completely ignores these issues, both of which have a dramatic effect on single-neuron and network behaviour.

In this paper, the current entering the soma from synaptic inputs along a dendritic tree will be computed as a function of the excitatory and inhibitory input firing rates The calculation can be applied to any dendritic geometry and any synaptic placements and it incorporates the full nonlinear effects of synaptic conductance changes. Several typical dendritic structures will be considered in detail and their impact on network dynamics will be discussed.

The unrealistic linear relation between input current and input firing rates used in neural network models has had a disastrous impact on their predictions. Due to extensive work on network associative memories [6, 7] (see [8, 9] for reviews), a great deal of interest has been focused on self-sustained firing patterns in neuronal populations. Network models based on linear excitation and inhibition predict that during such self-sustained firing, neurons will fire at their maximum possible rates. However, cortical neurons typically fire much more slowly than their maximum rates. Much attention has been given to finding a solution of this problem [10–17]. As discussed later, the firing rate problem is resolved when a realistic representation of synaptic inputs and a suitable dendritic geometry are included in the model.

To simplify the discussion, I will mainly consider a homogeneous population of neurons, that is a population in which all excitatory neurons fire at approximately the same rate. This will allow all of the issues concerning realistic conductance changes, dendritic geometry and population firing rates to be addressed. After the main points have been made, I will consider the case of an inhomogeneous population in which the spatially-structured firing patterns used in associative memory models can arise.

2. Mean-field theory and the firing rate problem

Consider a population of excitatory neurons firing at an average rate, $E(t)$, at time t. In the absence of external inputs, this firing rate is controlled by interconnections between the excitatory neurons in the population and by the effects of inhibitory interneurons. In the mean-field approach, the average firing rate for the population is related to the firing rate of a single neuron through the basic equation.

$$\frac{\mathrm{d}E}{\mathrm{d}t} = -E + F(I) \tag{2.1}$$

where $F(I)$ is a single-neuron firing rate as a function of input current I. If $F(I)$ is determined experimentally by injecting current into the soma, then in the natural setting the current I in equation (2.1) must be the current entering the soma due to

synaptic inputs For theoretical purposes, $F(I)$ is often assumed to have a sigmoidal form

$$F(I) = \frac{F_{max}}{1 + \exp[(\kappa - I)/\Delta]} \tag{2.2}$$

where F_{max} is the maximum firing rate for the neuron. The parameters κ and Δ correspond roughly to the threshold current and the width of the rise of the sigmoidal function. A firing rate F that is a threshold-linear function of I is probably more realistic over the relevant range of firing rates [17]. Both forms will be considered here.

In addition to the excitatory neurons described by the firing rate E, we must include a population of inhibitory interneurons. Let H represent the average firing rate of these inhibitory neurons. H is determined by an equation similar to (2.1). Since the analysis of the mean-field equation for H is identical to that for E, we will mainly concentrate on the equation for E. When a value for the inhibitory rate is needed (for graphs and specific examples) I will assume that the inhibitory rate H is proportional to the excitatory rate E. In the discussion, I will consider the mean-field equations for both E and H and show that this assumption is reasonable.

To complete the specification of the mean-field equations, we must determine how the current I depends on the excitatory and inhibitory firing rates E and H As discussed in the introduction, neural network models usually assume that I is a linear function of E and H. The assumed linear relation between input firing rates and input current leads to a firing rate disaster. The steady-state behaviour of a neuronal population described by mean-field theory can be determined by setting the time derivative in equation (2.1) to zero and demanding the self-consistent condition

$$E = F(I) \tag{2.3}$$

with I in turn written as a function of E and H. This equation just states that the average firing rate for the population agrees with the single-neuron rate. In figure 1 a graphical solution of equation (2.3) is constructed using the sigmoidal firing rate curve of equation (2.2). Solutions of (2.3) correspond to the three intersections of the straight line with the sigmoidal curve. The middle of these three solutions is unstable so only two states are relevant One is the silent state $E = 0$. Of particular interest is the other state representing stable self-sustained firing. Such self-sustained states have been used in models of memory [6, 7] and have been studied in great detail [8, 9]. However, while figure 1 indicates the existence of such a state it also points out the problem with it. The self-sustained firing state has a rate very near the maximum firing rate of a single neuron. Since recordings from the brain rarely detect neurons firing anywhere near their maximal firing rates, it is hard to argue that this state has anything to do with actual brain function.

Many suggestions have been made about how to get around the firing rate problem [10–17]. From this work it is known that nonlinear inhibition can solve the problem. Here, I will show how nonlinear inhibition arises as a natural consequence of correctly treating the shunting effects of synaptic inhibition along a dendritic cable.

3. Synaptic inputs and dendritic currents

To calculate how the somatic input current depends on the firing rates at excitatory and inhibitory synapses, we must assume some model for the neuron we consider. The

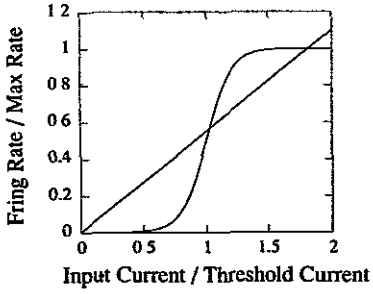

Figure 1. Graphical solution determining the average firing rate of a neuronal population. The sigmoidal curve is the single-neuron firing rate as a function of input current. The straight line is the result of the linear relation between input current and firing rate assumed in most neural network models. The inhibitory rate has been set equal to the excitatory rate. The two curves intersect at rates corresponding to a silent state, $E = 0$, an unstable intermediate state and a stable self-sustained firing state for which the firing rate is essentially the maximum single-neuron rate. The firing rate for this state is unrealistically high.

model neuron used throughout this discussion consists of an active soma and a single, passive dendritic tree. This arrangement is commonly known as the Rall model of the neuron [18, 19] and it has a long history in the literature [2, 3, 20–22]. The soma is considered to be the site of the nonlinear processes which result in the generation of an action potential and which determine the firing rate. (I will not distinguish between the soma and a nearby trigger zone on the axon, assuming that these are isopotential.) The dendritic tree is taken to have passive, voltage-independent membrane conductances. This is a fairly drastic approximation. However, even with a passive dendritic tree the nonlinear effects of synaptic conductances and dendritic geometry will be apparent and a passive dendritic model is sufficient both to incorporate these effects and to solve the firing rate problem. I will assume for simplicity that all synapses lie on the dendritic tree of the model neuron and not on its soma, although somatic inputs could easily be included. The general structure of the model neuron is shown in figure 2(a).

Since the synaptic inputs are located on the dendritic tree, the somatic input current I which determines the firing rate $F(I)$ is the current that enters the soma from the trunk of the dendritic tree (see figure 2(a)). Therefore, we must compute the current which flows out of the trunk of a dendritic tree into the soma when the dendritic membrane conductance is modified by synaptic excitatory and inhibitory inputs firing at rates E and H. The firing rates E and H are properties of the entire population so it is unlikely that they change appreciably over typical time scales corresponding to most dynamic processes within a single neuron. As a result the inputs governed by E and H are quasi-static on the scale of single neuron dynamics The quasi-static approximation is also justified by the fact that the time dependence of equation (2.1) is not intended to be realistic. The features modelled most accurately by the mean-field approach are, in fact, static.

Let $V(x)$ be the membrane potential at point x on an arbitrary dendritic tree We define the potential so that the membrane resting potential is zero. Thus, all other potentials are measured relative to the resting potential. The dendritic membrane conductance per unit area in the absence of synaptic inputs is denoted by g_m. Excitatory and inhibitory synapses along the dendritic tree produce conductance changes

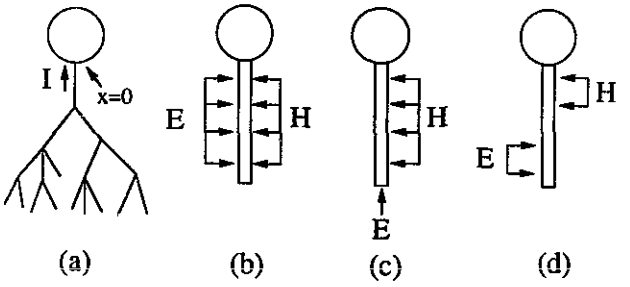

Figure 2. The model neurons considered. (*a*) The active soma and passive dendritic tree joined at the coordinate point $x = 0$. The current I to be computed is the current flowing from the dendritic tree into the soma (*b*), (*c*) and (*d*) The active soma with a single passive dendritic cable equivalent to the full tree in (*a*). For (*b*) excitatory and inhibitory synapses are uniformly distributed over the equivalent cable. In (*c*) excitatory synapses are located at the end of the cable and inhibitory synapses occur uniformly along its length. (*d*) shows an equivalent cable with excitatory synapses on the distal portion and inhibitory synapses spread over the proximal region.

that are proportional to the excitatory and inhibitory firing rates E and H We denote the conductance per unit area due to excitatory and inhibitory inputs at the point x by $c_e(x)E$ and $c_h(x)H$ respectively. The coefficients $c_e(x)$ and $c_h(x)$ depend on the density and strength of excitatory and inhibitory synapses at the point x. The membrane potential $V(x)$ is governed in the quasi-static case by the time-independent cable equation [23, 24]

$$\frac{a}{2r}\frac{d^2V}{dx^2} = g_m V + c_e E(V - V_e) + c_h H(V - V_h) \tag{3.1}$$

where a is the radius of the dendritic cable in the neighbourhood of the point x, r is the resistivity of the intracellular fluid and V_e and V_h are the reversal potentials for the excitatory and inhibitory synapses Typically, a is a few μm, $r \approx 100\ \Omega$ cm and V_e is around 75 mV. $V_h \approx 0$ for shunting inhibition and V_h is about -10 mV for hyperpolarizing inhibition.

Once equation (3 1) is solved for $V(x)$ the somatic input current can be found We choose the coordinate x as in figure 2(*a*) so that the soma joins the dendritic tree at the point $x = 0$. If the membrane potential at the soma is V_s then to ensure a continuous potential at $x = 0$ we must impose the boundary condition

$$V(0) = V_s \tag{3 2}$$

Additional boundary conditions are imposed at the branching nodes and at the points where the branches of the dendritic tree terminate [23, 24].

The current entering the soma from the dendritic tree can be obtained from $V(x)$ by noting that the current flowing longitudinally down a dendritic cable is given by the derivative of the voltage divided by the resistance of a unit length of cable,

$$I = \frac{\pi a_0^2}{r}\frac{dV}{dx}\bigg|_{x=0} \tag{3.3}$$

Here a_0 is the radius of the dendritic trunk. Once we have solved for $V(x)$, (3.3) gives us the desired formula for the input current I as a function of the firing rates E and H

Equation (3.1) is most easily solved if the synapses occur in bands of uniform density and strength so that c_e and c_h are piecewise constant functions. In this case, over any region of cable where c_e and c_h are constant $V(x)$ has the general form

$$V(x) = A_i \sinh(x/\lambda_i) + B_i \cosh(x/\lambda_i) + \bar{V}_i \tag{3.4}$$

where the index i labels the particular region being discussed. If region i has a cable radius a_i and constant synaptic density factors $c_e^{(i)}$ and $c_h^{(i)}$ then the cable length constant is given by

$$\lambda_i = \left(\frac{a_i}{2r(g_m + c_e^{(i)}E + c_h^{(i)}H)} \right)^{1/2} \tag{3.5}$$

and

$$\bar{V}_i = \frac{c_e^{(i)}EV_e + c_h^{(i)}HV_h}{g_m + c_e^{(i)}E + c_h^{(i)}H}. \tag{3.6}$$

Note that $\bar{V}_i$ and λ_i both depend on the firing rates E and H. The dependence of the length constant λ_i on the firing rates introduces the most dramatic nonlinearity into the relation between input current and firing rates.

The coefficients A_i and B_i are determined by imposing the boundary conditions consisting of (3.2) as well as continuity of the potential and current conservation at all junctions between regions and at all branching nodes on the tree. In addition, the appropriate boundary conditions must be satisfied at the terminals of the tree. If we label the region on the trunk of the dendritic tree nearest to the soma by $i = 0$ then the desired current entering the soma is

$$I = \frac{\pi a_0^2}{r\lambda_0} A_0. \tag{3.7}$$

Using these equations, the computation of the somatic input current as a function of E and H for any dendritic structure is merely a matter of algebra. However, for highly structured dendritic trees the algebra can be tedious and the answers quite complicated. The tedium and complexity are dramatically reduced if we make use of a very convenient simplification due to Rall [20, 23]. The idea is to replace a complete dendritic tree with a single cylindrical cable having the same total electrotonic length as the original tree and the same total surface area. The electrotonic length is computed by summing the lengths of the various segments of the tree measuring each segment length in units of its length constant λ_i. This reduction is exact if the geometry of the dendritic tree satisfies three requirements:

(i) the electrotonic length is the same from the soma to all terminals of the tree;
(ii) at a node where a single dendritic cable segment breaks into several branches, the sum of the $\frac{3}{2}$ power of the radii of each of the branches is equal to the $\frac{3}{2}$ power of the radius of the original cable segment; and
(iii) regions of the dendritic tree at equal electrotonic distances from the soma receive equal synaptic inputs.

Even if these requirements are not exactly satisfied the equivalent cable is a reasonable approximation.

We now compute $I(E, H)$ for a single equivalent cable of radius a and length L considering several different synaptic placements. First, imagine that the excitatory and inhibitory synapses are uniformly spread along the entire dendritic cable as in figure 2(b). In this case, the synaptic density and strength factors c_e and c_h are constants and we only need a single region corresponding to $i = 0$. In this example, no current flows in or out of the end of the cable at $x = L$ so we require the boundary condition.

$$\left.\frac{dV}{dx}\right|_{x=L} = 0. \tag{3.8}$$

The cable length constant for this case is

$$\lambda = \left(\frac{a}{2r(g_m + c_e E + c_h H)}\right)^{1/2} \tag{3.9}$$

and the input current for the geometry of figure 2(b) given by these formulae is

$$I = 2\pi a\lambda[-g_m V_s + c_e E(V_e - V_s) + c_h H(V_h - V_s)]\tanh(L/\lambda). \tag{3.10}$$

For a short cable $L \ll \lambda$, this formula is, in fact, linear in E and H,

$$I \approx 2\pi a L[-g_m V_s + c_e E(V_e - V_s) + c_h H(V_h - V_s)] \tag{3.11}$$

Note that this is just the area of the cable times the input current density. However, the cable length is typically not much shorter than the length constant even when $E = H = 0$ but instead L is of order λ. In any case, as the firing rates E and H increase the cable length constant, which is inversely proportional to the square root of $g_m + c_e E + c_h H$, gets smaller and eventually it will become considerably less than L. At this point the current (3.10) grows only like $E^{1/2}$ for large E. Thus, even for this trivial geometry we see that cable effects produce a nonlinear dependence on firing rates and reduce the growth of I with E.

The nonlinear dependence of I on the firing rates is more dramatic if the excitatory and inhibitory inputs are segregated along the cable. To keep the following expressions as simple as possible we will consider this case when the membrane potential of the soma is equal to the resting potential, $V_s = 0$. In addition, we take the inhibitory synapses to be of the shunting type so that $V_h = 0$ as well. The first synaptic placement we consider is that of excitatory synapses located at the end of the equivalent cable at $x = L$ and shunting inhibitory synapses located uniformly all along the equivalent cable. This geometry is shown in figure 2(c). The calculation is almost identical to the previous case except that the boundary condition at the end of the cable is now

$$\left.\frac{dV}{dx}\right|_{x=L} = rc_e E[V_e - V(L)] \tag{3.12}$$

and the cable length constant is

$$\lambda = \left(\frac{a}{2r(g_m + c_h H)}\right)^{1/2}. \tag{3.13}$$

Note how increased inhibitory firing decreases the size of this length constant. The resulting somatic current for the synaptic connections shown in figure 2(*c*) is

$$I = \frac{\pi a^2 c_e E V_e}{\cosh(L/\lambda) + r\lambda c_e E \sinh(L/\lambda)}. \tag{3.14}$$

In the limit of short cable length $L \ll \lambda$, this becomes

$$I \approx \frac{\pi a^2 c_e E V_e}{1 + r c_e E L}. \tag{3.15}$$

In this limit, we see that for high excitatory firing rates the current approaches a finite limiting value

$$I \to \frac{\pi a^2 V_e}{rL} \tag{3.16}$$

which is just the value given by Ohm's law for the cable. However, typically $L \approx \lambda$ in the absence of inhibitory inputs and $L > \lambda$ when the inhibitory inputs are firing. Then the nonlinear effects of inhibition become even more pronounced The current (3.14) is plotted in figure 3 assuming $c_e E = c_h H$ with typical values of the cable parameters (Choosing $c_e E = c_h H$ means that a relatively small amount of current enters through the excitatory inputs since these are restricted to the end of the cable. However, increasing c_e does not drastically change the shape of the curve in figure 3, it mainly increases the overall amplitude of the current) Note that for high firing rates the current turns over and goes ultimately to zero

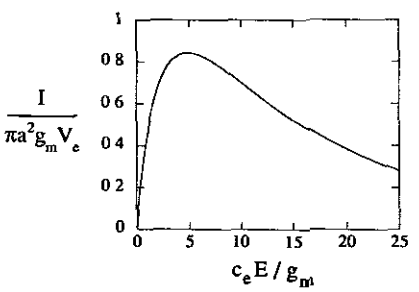

Figure 3. The input current as a function of excitatory rate for the geometry of figure 2(*c*) The excitatory and inhibitory synaptic conductances have been set equal to each other Note that the nonlinear effect of shunting inhibition causes the input current to reach a maximum value and then to decrease with increased input firing

The result (3.14) is well fitted by an approximate formula

$$I = \alpha E \exp(-\beta\sqrt{H}) \tag{3.17}$$

with α and β constants It is easy to see where such a form comes from. The linear dependence in the excitatory rate is just what has always been used in network models. When a current propagates down a cable of length of L it is, roughly speaking, reduced by a factor $\exp(-L/\lambda)$ The form (3.17) follows from the fact that when shunting

inhibition is large enough to significantly modify the total membrane conductance, the cable length constant λ is proportional to the inverse of the square root of the inhibitory rate. The exponential dependence in (3.17) shows the highly nonlinear effect of shunting inhibition.

As a final example, we consider the case shown in figure 2(d) where uniform shunting inhibitory synapses are located in the region $0 \leqslant x \leqslant L_0$ and excitatory synapses in the region $L_0 < x \leqslant L$. We impose the no-current boundary condition at $x = L$ and $V_s = 0$. The resulting current is

$$I = \frac{2\pi a \lambda_1 c_e E V_e \tanh[(L - L_0)/\lambda_1]}{\cosh(L_0/\lambda_0) + \lambda_0/\lambda_1 \sinh(L_0/\lambda_0)\tanh[(L - L_0)/\lambda_1]} \tag{3.18}$$

where

$$\lambda_0 = \left(\frac{a}{2r(g_m + c_h H)}\right)^{1/2} \tag{3 19}$$

and

$$\lambda_1 = \left(\frac{a}{2r(g_m + c_e E)}\right)^{1/2} \tag{3.20}$$

This result if clearly more complicated than the previous ones However, it still has the basic shape of the result shown in figure 3 and can be approximated with an expression of the form (3 17). In particular, it shows the exponential suppression of the current for large inhibitory firing rates.

4. Results from a realistic model neuron

To verify that these results are relevant for realistic neurons, I have performed simulations of a multi-compartmental neuron model based on measured active membrane conductances. The model used for simulations has an active soma compartment and ten passive compartments forming an equivalent dendritic cable. The active conductances are a transient sodium conductance, a delayed-rectifier potassium conductance and a transient potassium conductance. The form and dynamics used for these conductances is exactly as measured in [25] The transient sodium and delayed-rectifier conductances are needed to generate action potentials while the transient potassium conductance is required to obtain a realistic firing rate as a function of injected current. The presence of the transient potassium current allows the model neuron to repetitively fire at arbitrarily slow rates for input currents near the threshold value. This model is the simplest conductance-based model which gives a firing rate curve that rises continuously from zero

Synaptic inputs are included in the model by changing the membrane conductances in the various dendritic compartments receiving synaptic inputs. Each input spike results in a transient conductance change given by the difference of two exponentials For these simulations the synaptic rise time was 1 ms or less and the decay time was in the range of 1–10 ms. The results are not very sensitive to the values used for the synaptic time constants. The length of the equivalent dendritic cable was three-quarters of a length constant in the absence of synaptic inputs Excitatory synaptic

conductance changes were introduced into the distal three compartments and shunting synaptic inputs affected the proximal seven compartments of the dendritic cable. Thus the arrangement is similar to figure 2(*d*). The inhibitory and excitatory input rates were set equal to each other The input rate for simulation runs is defined to be the total number of inputs per unit time along the entire dendritic cable and thus is larger than any single-neuron rate.

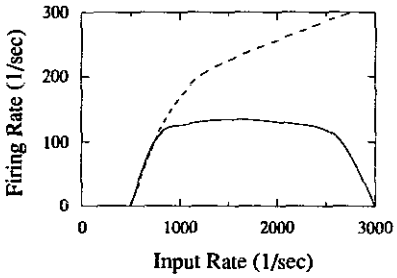

Figure 4. The firing rate as a function of excitatory input rate for a multicompartmental model neuron based on realistic conductances [25] The input rate shown refers to the sum of all inputs synapsing on the dendritic cable, not to a single-neuron rate. The broken curve is the firing rate in the absence of inhibition while the full curve corresponds to shunting inhibition with the inhibitory firing rate proportional to the excitatory rate. In the presence of inhibition, the firing rate reaches a maximum and then decreases to zero as the input rate is increased.

The results of the simulation runs are shown in figure 4 The broken curve shows the firing rate as a function of input rate in the absence of shunting inhibition The curve rises linearly at first and then continues to rise more slowly. The solid curve shows the firing rate including shunting. As predicted by the results of the previous section, the firing rate reaches a maximum value and then decreases. Shunting has the nonlinear effect predicted and is able to bound the firing rate well below its maximum value. The firing rate has a plateau at about 100 Hz. This could be reduced more by increasing the magnitude of the transient potassium conductance or by including additional currents that produce spike rate adaptation (see, for example, [26-27]. However, the model as shown clearly exhibits the nonlinear inhibitory effects we are discussing.

5. Firing rates in a population with shunting inhibition

To see how the input currents we have computed resolve the firing rate problems, we solve equation (2.3) for the static firing rate using the firing rate function (2.2) but this time with the result of equation (3.14) for the input current as a function of firing rate. Again we taken $c_e E = c_h H$ A graphical solution is shown in figure 5. There are three solutions corresponding to places where the two lines cross, but only the solutions at $E = H = 0$ and at the right-most crossing are stable. As in figure 1, there exists a self-sustained firing state but now the rate is well below the maximum firing rate for the neuron. The same firing rate curve was used in figure 5 as in figure 1, the difference is solely the result of nonlinear shunting inhibition. It is interesting to note that as the self-sustained state is approached from the left in figure 5, the firing rate actually decreases after first passing through a maximum.

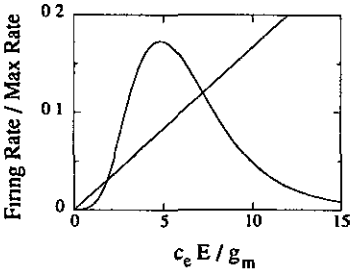

Figure 5. Graphical solution determining the average firing rate of a neuronal population. The curve is the single-neuron firing rate as a function of input rate using the nonlinear expression for the dendritic geometry of figure 2(*c*) This curve meets the straight line at places where a static solution of the mean-field equations exist One intersection corresponds to the silent state $E = 0$ The intermediate crossing is unstable and the upper intersection represents a stable self-sustained firing state for which the firing rate is significantly lower than the maximum single-neuron rate.

6. Discussion

Within the cable literature there are analyses of the impact of synaptic conductance on the time and length constants of dendritic cables [2, 3, 20-22]. The main message of this paper is that the effects of dendritic geometry, synaptic placements and synaptic conductances can be included in mean-field-based network models For example, shunting inhibition along the length of a dendritic cable through which excitatory signals must pass results in an exponential suppression of the firing rate This result can be approximated by relation (3 17). In the discussion to this point, I have used the standard sigmoidal firing rate curve of equation (2.2). However, as can be seen by the broken curve in figure 4, in the low-rate region a threshold-linear function is more appropriate,

$$F(I) = [I - \kappa]\Theta[I - \kappa] \tag{6 1}$$

where κ is the threshold current and Θ is a unit step function The units of the current I have been chosen so that the multiplicative constant in equation (6.1) is unity. The threshold linear form cannot be used in models which assume a linear dependence of the current on the firing rates since these models rely on the firing rate maximum of the sigmoidal function to prevent arbitrarily high rates. Now that we have resolved the firing rate problem, we can use the simpler and more realistic threshold-linear form.

Up to now the dynamics of the inhibitory rate H has not been considered. H obeys an equation similar to (2.1) and two, coupled differential equations describe the combined system. Suppose that the inhibitory neurons shunt the dendritic cables of the excitatory neurons but not each other, and that the inhibitory neurons are excited by the E neurons. The dendritic geometry for excitatory neurons is as in figures 2(*c*) or 2(*d*) so that the fit of equation (3.17) is applicable. For inhibitory neurons I take a geometry as in figure 2(*b*) except that there are no inhibitory synapses. I assume that for the inhibitory neurons $g_m > c_e E$ over the range of interest so that the excitatory input is approximately linear for these neurons, $I = \gamma E$. This is not essential but it simplifies the resulting equations. Finally, I use the threshold-linear firing rate curve

(6.1). The coupled equations describing the system are then

$$\frac{dE}{dt} = -E + (\alpha E \exp(-\beta\sqrt{H}) - \kappa_e)\Theta[\alpha E \exp(-\beta\sqrt{H}) - \kappa_e] \qquad (6\ 2)$$

and

$$\tau_h \frac{dH}{dt} = -H + (\gamma E - \kappa_h)\Theta[\gamma E - \kappa_h]. \qquad (6.3)$$

We have included the time constant τ_h to allow for the possibility that the inhibitory neurons respond at a different rate from the excitatory ones. Note that if the inhibitory threshold current κ_h is small the asymptotic value of the inhibitory rate is proportional to the excitatory rate as we have assumed in previous sections.

Static solutions of the coupled equations for E and H can be found by plotting nullclines in the E–H plane. These are lines along which either $dE/dt = 0$ or $dH/dt = 0$. This is done in figure 6. In addition to the silent state $E = H = 0$, static solutions are given by the intersections of the two nullclines. Again only the rightmost intersection point is stable and we find a self-sustained firing state similar to that of figure 5.

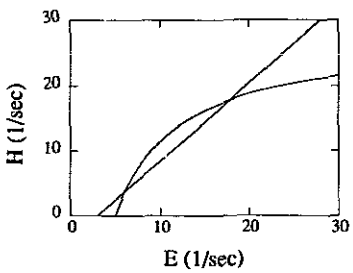

Figure 6. Nullclines for the coupled system of equations describing the dynamics of both excitatory and inhibitory neurons. The intersections of the two curves as well as the point $E = H = 0$ are the static states as discussed in the caption of figure 5.

In neural network models, spatially structured patterns of self-sustained firing are used as memory states [5–9]. To describe such patterns we must include a set of N variables E_i and H_i which are the average excitatory and inhibitory firing rates in a spatial region labelled by the index $i = 1, 2 \ldots, N$. These regions may correspond to small populations or even single neurons. The excitatory regions are coupled to each other with variable strength. The strength of the synapse coupling region j to region i is given by the matrix element J_{ij}. In addition the excitatory neurons in region i couple locally to inhibitory interneurons in that region and the inhibitory neurons shunt the excitatory neurons in the region but not each other. Clearly this is just one of many possible arrangements. The network is described by the $2N$ equations

$$\frac{dE_i}{dt} = -E_i + \left(\alpha \sum_{j=1}^{N} J_{ij} E_j \exp(-\beta\sqrt{H_i}) - \kappa_e\right) \Theta \left[\alpha \sum_{j=1}^{N} J_{ij} E_j \exp(-\beta\sqrt{H_i}) - \kappa_e\right] \qquad (6.4)$$

and

$$\tau_h \frac{dH_i}{dt} = H_i + (\gamma E_i - \kappa_h)\Theta[\gamma E_i - \kappa_h]. \tag{6.5}$$

These equations can be simplified if in the time units we are using $\tau_h \ll 1$. Then the inhibitory neurons respond more quickly than the excitatory neurons and we can set the H_i equal to their asymptotic values. For small inhibitory thresholds this means we can take $H_i \approx \gamma E_i$. Then the $2N$ equations are replaced by N equations.

$$\frac{dE_i}{dt} = -E_i + \left(\alpha \sum_{j=1}^{N} J_{ij} E_j \exp(-\beta' \sqrt{E_i}) - \kappa_e\right) \Theta \left[\alpha \sum_{j=1}^{N} J_{ij} E_j \exp(-\beta' \sqrt{E_i}) - \kappa_e\right] \tag{6.6}$$

where $\beta' = \beta(\gamma)^{1/2}$ Using either the $2N$ or the simplified N equations these models represent a neural network with associative memory properties and a well regulated firing rate. The model of equations (6.4) and (6.5) has been simulated and shown to provide associative recall of stored memory firing patterns with stable, low firing rates [28].

I have concentrated mostly on dendritic geometries like those of figure 2(c) or 2(d) because they clearly illustrate the nonlinear effect of shunting along a cable However, the formalism developed here allows any dendritic structure with any placements of excitatory and inhibitory synapses to be included in network models This will permit studies of the effect of dendritic and synaptic geometry on network behaviour.

Acknowledgments

I wish to thank Dani Amit, Alessandro Treves, Eve Marder, John Rinzel and Wil Rall for helpful comments and encouragement. This research has been supported by Department of Energy contract DE-AC0276-ER03230 and by National Institute of Mental Health grant MH46742.

References

[1] Wilson H R and Cowan J D 1974 Excitatory and inhibitory interactions in localized populations of model neurons *Biophys. J.* **12** 1

[2] Rall W 1964 Theoretical significance of dendritic trees for neuronal input–output relations *Neural Theory and Modeling* ed R Reiss (Stanford, CA: Stanford University Press) pp 73–97

[3] Jack J J B, Noble D and Tsien R W 1975 *Electrical Current Flow in Excitable Cells* (Oxford. Oxford University Press)

[4] Segev I and Parnas I 1989 Synaptic integration mechanisms: a theoretical and experimental investigation of temporal postsynaptic interaction between excitatory and inhibitory input *Biophys. J* **41** 41

[5] Koch C, Poggio T and Torre V 1983 Nonlinear interactions in a dendritic tree: localization, timing and role in information processing *Proc. Natl Acad. Sci. USA* **80** 2799

[6] Hopfield J J 1982 Neural networks and systems with emergent selective computational abilities *Proc. Natl Acad. Sci. USA* **79** 2554

[7] Little W A 1974 The existence of persistent states in the brain *Math. Biosci.* **19** 101

[8] Amit D J 1989 *Modelling Brain Function* (Cambridge: Cambridge University Press)

[9] Hertz J 1990 *Introduction to the Theory of Neural Computation* (Reading, MA: Addison-Wesley)

[10] Amit D J and Treves A 1989 Associative memory neural networks with low temporal spiking rates *Proc. Natl Acad Sci. USA* **86** 7671

[11] Treves A and Amit D J 1989 Low firing rates: an effective Hamiltonian for excitatory neurons *J Phys. A: Math. Gen.* **22** 2205

[12] Rubin N and Sompolinsky H 1989 Neural networks with low local firing rates *Europhys. Lett.* **10** 465

[13] Buhmann J 1989 Oscillations and low firing rates in associative memory neural networks *Phys. Rev.* A **40** 4145

[14] Golomb D, Rubin N and Sompolinsky H 1990 The Willshaw model: Associative memory with sparse coding and low firing rates *Phys. Rev.* A **41** 1843

[15] Amit D J, Evans M R and Abeles M 1990 Attractor neural networks with biological probe records *Network* **1** 381

[16] Amit D J and Tsodyks M V 1991 Quantitative study of attactor neural network retrieving at low spike rates I: Substrate—spikes, rates and neuronal gain *Network* in press

[17] Treves A 1990 Threshold-linear formal neurons in auto-associative nets *J. Phys. A. Math. Gen.* **23** 2418

—— 1990 Graded-response neurons and information encodings in auto-associative memories *Phys. Rev.* A **42** 2418

[18] Rall W 1959 Branching dendritic trees and motoneuron membrane resistivity *Exp. Neurology* **1** 491

[19] Rall W and Shepherd G S 1968 Theoretical reconstruction of field potentials and dendrodendritic synaptic interaction in olfactory bulb *J. Neurophysol.* **30** 884

[20] Rall W 1962 Theory of physiological properties of dendrites *Ann. NY Acad. Sci.* **96** 1071

[21] Holmes W R and Woody C D 1988 The effectiveness of individual synaptic inputs with uniform and nonuniform patterns of background synaptic activity *Cellular Mechanism of Conditioning and Behavioral Plasticity* ed C D Woody, D Alkon and J McGaugh (New York: Plenum) p 345

[22] Holmes W R and Woody C D 1989 Effects of uniform and nonuniform synaptic activation-distributions on the cable properties of modeled cortical pyramidal neurons *Brain Res.* **505** 12

[23] Rall W 1977 Core conductor theory and cable properties of neurons *Handbook of Physiology Vol. 1* ed E R Kandel (Bethesda, MD: American Physiological Society)

[24] Tuckwell H C 1988 *Introduction to Theoretical Neurobiology* (Cambridge: Cambridge University Press)

[25] Connor J A, Walter D and McKown R 1977 Neural repetitive firing: Modifications of the Hodgkin–Huxley axon suggested by experimental results from crustacean axons *Biophys. J.* **18** 81

[26] Yamada W M, Koch C and Adams P R 1989 Multiple channels and calcium dynamics *Methods of Neuronal Modeling* ed C Koch and I Segev (Cambridge, MA: MIT Press)

[27] McCormick D A 1990 Membrane properties and neurotransmitter actions *The Synaptic Organization of the Brain* ed G M Shepherd (Oxford: Oxford University Press)

[28] Abbott L F 1991 A firing rate model of neuronal populations in the neocortex *Neural Networks: From Biology to High-Energy Physics* to be published